Title 論文題目	Type 2 diabetes induces subendocardium-predominant reduction in transient outward K^+ current with downregulation of Kv4.2 and KChIP2. (2 型糖尿病は心内膜側優位に Kv4.2 と KChIP2 の発現を低下させることにより一過性外向きカリウム電流の減少を引き起こす)
Author(s) 著　者	佐藤, 達也
Degree number 学位記番号	乙第 2922 号
Degree name 学位の種別	博士（医学）
Issue Date 学位取得年月日	2017-02-06
Original Article 原著論文	American Journal of Physiology - Heart and Circulatory Physiology 2014; 306: H1054-1065
Doc URL	
DOI	
Resource Version	

Am J Physiol Heart Circ Physiol 306: H1054–H1065, 2014.
First published January 31, 2014; doi:10.1152/ajpheart.00414.2013.

Type 2 diabetes induces subendocardium-predominant reduction in transient outward K^+ current with downregulation of Kv4.2 and KChIP2

Tatsuya Sato,[1,2] Takeshi Kobayashi,[1] Atsushi Kuno,[2,3] Takayuki Miki,[2] Masaya Tanno,[2] Hidemichi Kouzu,[2] Takahito Itoh,[2] Satoko Ishikawa,[2] Takashi Kojima,[4] Tetsuji Miura,[2] and Noritsugu Tohse[1]

[1]*Department of Cellular Physiology and Signal Transduction, Sapporo Medical University School of Medicine, Sapporo, Japan;* [2]*Department of Cardiovascular, Renal and Metabolic Medicine, Sapporo Medical University School of Medicine, Sapporo, Japan;* [3]*Department of Pharmacology, Sapporo Medical University School of Medicine, Sapporo, Japan; and* [4]*Department of Cell Science, Research Institute of Frontier Medicine, Sapporo Medical University School of Medicine, Sapporo, Japan*

Submitted 17 May 2013; accepted in final form 27 January 2014

Sato T, Kobayashi T, Kuno A, Miki T, Tanno M, Kouzu H, Itoh T, Ishikawa S, Kojima T, Miura T, Tohse N. Type 2 diabetes induces subendocardium-predominant reduction in transient outward K^+ current with downregulation of Kv4.2 and KChIP2. *Am J Physiol Heart Circ Physiol* 306: H1054–H1065, 2014. First published January 31, 2014; doi:10.1152/ajpheart.00414.2013.—In the present study, we examined if and how cardiac ion channels are modified by type 2 diabetes mellitus (T2DM). Subendocardial (Endo) myocytes and subepicardial (Epi) myocytes were isolated from left ventricles of Otsuka-Long-Evans-Tokushima Fatty rats (OLETF) rats, a rat model of T2DM, and Otsuka-Long-Evans-Tokushima (LETO) rats (nondiabetic control rats). Endo and Epi myocytes were used for whole cell patch-clamp recordings and for protein and mRNA analyses. Action potential durations in Endo and Epi myocytes were longer in OLETF rats than in LETO rats, and the difference was larger in Endo myocytes. Steady-state transient outward K^+ current (I_{to}) density was reduced in Endo but not Epi myocytes of OLETF rats compared with LETO rats, although the contribution of the fast component of I_{to} recovery from inactivation was smaller in both Endo and Epi myocytes of OLETF rats than in LETO rats. Kv4.2 protein was reduced only in Endo myocytes in OLETF rats, although voltage-gated K^+ channel-interacting protein 2 (KChIP2) protein levels in both Endo and Epi myocytes were lower in OLETF rats than in LETO rats. Corresponding regional differences in mRNA levels of KChIP2 and Kv4.2 were observed between OLETF and LETO rats. mRNA levels of Iroquois homeobox 5 in Endo myocytes were 53% higher in OLETF rats than in LETO rats. Densities of inward rectifier K^+ current and L-type Ca^{2+} current and mRNA levels of Kv4.3 and Kv1.4 were similar in OLETF and LETO rats. In conclusion, T2DM induces Endo-predominant prolongation of the action potential duration via a reduction of the fast component of I_{to} recovery from inactivation and reduced steady-state I_{to}, in which downregulation of Kv4.2 and KChIP2 may be involved. Increased Iroquois homeobox 5 expression may underlie Kv4.2 downregulation in T2DM.

cardiac ion channel remodeling; Iroquois homeobox 5; voltage-gated K^+ channel-interacting protein 2; Kv4.2; type 2 diabetes

DIABETES MELLITUS (DM) is associated with not only atherosclerotic vascular events but also a high risk of nonischemic ventricular dysfunction, so-called "diabetic cardiomyopathy" (18). Diabetes is one of the diseases underlying heart failure with preserved left ventricular (LV) ejection fraction (2), and the prognosis of heart failure has been shown to be substantially worsened by diabetes. A number of studies in the past two decades have disclosed abnormalities in the microcirculation, mitochondria, and metabolism in diabetic hearts, as recently reviewed elsewhere (18). However, knowledge of electrical remodeling in the heart by type 2 DM (T2DM) is very limited. Most of the earlier studies used models of type 1 DM (T1DM; i.e., streptozotocin-induced and alloxan-induced diabetes) and showed that the action potential (AP) duration (APD) was prolonged and that the transient outward K^+ current (I_{to}), L-type Ca^{2+} current ($I_{Ca,L}$), and inward rectifier K^+ current (I_{K1}) were reduced in T1DM (31, 38, 45). However, it remains unclear whether T2DM induces the same electrical remodeling as that induced by T1DM. Hyperglycemia is a common feature in all animal models of diabetes, but plasma levels of insulin and lipids are different in T1DM and T2DM and also in models of T2DM (28, 44). In addition, characteristics of LV pressure-volume relationship are different in T1DM and T2DM (25), indicating a possible difference in modifications of excitation-contraction coupling between the two types of DM.

In the present study, we aimed to characterize the influence of T2DM on APD and ion currents in cardiomyocytes. We used Otsuka-Long-Evans-Tokushima-Fatty (OLETF) rats, as a model of T2DM, and their nondiabetic controls, Otsuka-Long-Evans-Tokushima (LETO) rats. OLETF rats lack the cholecystokinin-A receptor, which regulates appetite, and spontaneously develop hyperphagia, obesity, hyperglycemia, hypertriglyceridemia, hyperinsulinemia, and mild hypertension (19, 27, 44). Metabolic features of OLETF rats and mild hypertension at 25~30 wk of age were confirmed in our previous studies showing a reduction in end-diastolic ventricular elastance with preserved end-systolic ventricular elastance (35) and enlargement of infarct size after ischemia-reperfusion (17). Considering the transmural difference in electrophysiological properties in the ventricle, we examined the kinetics of ion channel currents and mRNA and protein expression levels of ion channel subunits separately in the subendocardial (Endo) and subepicardial (Epi) myocardium.

METHODS

Animal preparation. This study was conducted in accordance with the National Institutes of Health *Guide for the Care and Use of Laboratory Animals* (NIH Pub. No. 85-23, Revised 1996), and all animal experiments were approved by the Animal Use Committee of Sapporo Medical University. Male OLETF and LETO rats at 25–30

Address for reprint requests and other correspondence: T. Sato, Sapporo Medical Univ. School of Medicine, South-1 West-17, Chuo-ku, Sapporo 060-8556, Japan (e-mail: satatsu.bear@gmail.com).

wk of age were analgesized with buprenorphine (0.03 mg/kg ip) and anesthetized with pentobarbital sodium (80 mg/kg ip). The adequacy of anesthesia was determined by a negative toe pinch reflex, and the chest was then opened for isolation of the heart.

Myocyte isolation. Isolation of myocytes from rat hearts was performed as previously described with slight modifications (36). Briefly, the heart was quickly excised from the open-chest rat and was retrogradely perfused in a Langendorff apparatus with normal Tyrode solution containing (in mmol/l) 143 NaCl, 5.4 KCl, 0.5 $MgCl_2$, 1.8 $CaCl_2$, 0.33 NaH_2PO_4, 5.5 glucose, and 5.0 HEPES (pH adjusted to 7.4 with NaOH). The perfusate was oxygenated with 100% O_2 and kept at 37°C. After 10 min of perfusion with normal Tyrode solution, the perfusate was changed to Ca^{2+}-free Tyrode solution for 20 min. The heart was then perfused with Ca^{2+}-free Tyrode solution containing 0.3 mg/ml collagenase (Wako Chemicals, Osaka, Japan) for 35 min, and the LV was removed and placed in Kraftbrühe solution containing (in mmol/l) 40 KCl, 3.0 $MgCl_2$, 20 KH_2PO_4, 50 L-glutamic acid, 20 taurine, 10 glucose, 0.5 EGTA, and 10 HEPES (pH adjusted to 7.4 with KOH). Small pieces of LV free wall tissues were dissected from the Endo and Epi surfaces (to a depth not exceeding 10% of the thickness of the ventricular wall) using fine scissors, and Endo and Epi tissues were used for the isolation of Endo and Epi myocytes, respectively. The dissected tissue pieces were suspended in Kraftbrühe solution, gently stirred, and filtered through a 100-μm pore stainless steel mesh. The cell suspension was stored in a refrigerator (4°C). Isolated myocytes were used at 1–7 h after isolation.

Patch-clamp recording. Whole cell patch-clamp recordings were performed using a patch-clamp amplifer (Axopatch 200B, Axon Instruments, Union City, CA) according to standard techniques with slight modifications as previously described (36). Patch pipettes had tip resistances of 3–4 MΩ for AP recording and 2–3 MΩ for ionic current recording. Cells were placed in a perfusion chamber (1 ml in volume) and constantly superfused with external solutions at 37°C.

APs were recorded in the current-clamp mode. As in our previous studies (12, 20), the internal solution contained (in mmol/l) 20 KCl, 110 L-asparate, 1.0 $MgCl_2$, 5.0 K_2-ATP, 5.0 creatine phosphate-K_2, 5.0 EGTA, and 5.0 HEPES (pH of the solution was adjusted to 7.4 with KOH). The final concentration of K^+ in the internal solution determined by a radiometer was 152 mmol/l. The external solution was normal Tyrode solution. To determine the stimulation current, APs were evoked by brief (0.5 ms) currents of 1–20 nA at 1-s intervals. Stimulation currents were defined by the next current of threshold current. APs were evoked by stimulation currents at 1 Hz 15 times. APDs were measured at 25%, 50%, and 90% repolarization (APD_{25}, APD_{50}, and APD_{90}, respectively). Steady-state APD was defined as APD at the 15th stimulation. In addition to 1 Hz, 4 Hz was tried as the frequency of stimulation in preliminary experiments, but it often induced cell death, possibly as a result of Ca^{2+} overload, and thus was not selected in this study.

Voltage-clamp experiments were performed to record ionic currents. For recording K^+ currents, the internal solution was the same as that used for the current-clamp experiments. The external solution contained (in mmol/l) 143 choline Cl, 5.4 KCl, 0.5 $MgCl_2$, 2.0 $CoCl_2$, 5.5 glucose, and 5.0 HEPES (pH adjusted to 7.4 with Tris). To eliminate Na^+ current (I_{Na}) and Ca^{2+} current, NaCl was replaced with choline Cl and $CaCl_2$ was replaced with $CoCl_2$ in the external solution. We selected Co^{2+} to block $I_{Ca,L}$ since Co^{2+} eliminated $I_{Ca,L}$ in rat ventricular myocytes without any major effects on I_{to} in our previous study (37). I_{to} was elicited by a series of 300-ms test potentials from −40 to +50 mV from a holding potential of −80 mV. I_{to} was determined by subtracting the sustained outward current (I_{ss}) from the peak outward current (I_{peak}). I_{to} was determined also as a current sensitive to a high concentration (3 mM) of 4-aminopyridine (4-AP; Wako Chemicals, Osaka, Japan), as previously reported (43). In addition, we examined currents sensitive to a low concentration (50 μM) of 4-AP, which represents slow inactivation kinetics (43, 47). Recovery of I_{to} ($I_{peak} - I_{ss}$) from inactivation was examined by a double-pulse protocol with voltage steps from −80 to +50 mV and an interval varying from 1 to 3,000 ms. Since the I_{to} recovery process consists of at least two components (11, 12), the process was fitted with a two-component exponential function.

I_{K1} was elicted by voltage steps from −110 to −40 mV from a holding potential of −80 mV. I_{K1} was determined by current densities at 300 ms from the start of voltage steps. For recording $I_{Ca,L}$, a Cs^+-rich internal solution was used to isolate $I_{Ca,L}$. The internal solution contained (in mmol/l) 20 CsCl, 110 L-asparate, 1.0 $MgCl_2$, 5.0 Mg-ATP, 5.0 creatine phosphate-Na_2, 10 EGTA, and 5.0 HEPES (pH adjusted to 7.4 with CsOH). The Ca^{2+} concentration in the internal solution was not directly measured but was presumably kept negligibly low by EGTA. The external solution contained (in mmol/l) 143 choline Cl, 5.4 CsCl, 0.5 $MgCl_2$, 1.8 $CaCl_2$, 5.5 glucose, and 5.0 HEPES (pH adjusted to 7.4 with Tris). $I_{Ca,L}$ was elicited by a series of 300-ms test potentials from −60 to +50 mV from a holding potential of −90 mV. Pipette capacitance compensation was not used to obtain an accurate current-voltage relation. All liquid junction potentials (−10 mV) were compensated. Current signals were filtered at 2 kHz and digitized at 10 kHz. Current amplitudes were normalized to cell capacitance to correct for different cell sizes.

RNA preparation and quantitative RT-PCR. RNA was extracted from tissue samples and analyzed as previously reported (9, 35). In brief, Endo and Epi tissues were carefully sampled with sharp scissors in cold (4°C) Tyrode solution in a refrigerator room. Tissues were frozen in liquid nitrogen and stored at −80°C. Total RNA was extracted from frozen myocardial tissue samples using an RNeasy Mini Kit (Qiagen, Germantown, MD) according to the manufacturer's instructions. Quantitative RT-PCR was performed on a StepOne RT-PCR system (Applied Biosystems) using either Taqman Universal Master Mix or Power SYBR green Master Mix, depending on target genes. The following Taqman probes were used: *KCND2* (Kv4.2), Rn00581941_m1; *KCND3* (Kv4.3), Rn01534234_m1; *KCNA4* (Kv1.4), Rn02532059_s1; Iroquois homeobox 5 (*Irx5*), Rn01538194_m1; and β-actin (*ActB*), Rn00667869_m1. Primer sequences were as follows: *KCNE4* (MiRP3), 5′-TGGAAGGGGATAGTGTGAGC-3′ and 5′-TGTAGACCCTTCGCTGCTTT-3′; *KCNIP2* [voltage-gated K^+ channel-interacting protein 2 (KChIP2)], 5′- GCTACTTTTCTCTTCAATGCCTT-3′ and 5′-AAACCAGCCACAAAGTCCTCAA-3′; *SCN5A* (Nav1.5), 5′-TCTTCGACAGCATCATCGTC-3′ and 5′-GACTTGGCCAGCTTGAAGAC-3′; and Iroquois homeobox 4 (*Irx4*), 5′-TGCTGATGGAGCTGTTATGG-3′ and 5′-TGGTGCCTATCCAGAGTTCC-3′. Differences between mRNA levels were examined by the comparative threshold cycle method. β-Actin was used as an endogenous control.

Immunoblot analysis. Myocardial tissues from Endo and Epi regions of the LV were minced in ice-cold mannitol-sucrose-EGTA buffer containing (in mmol/l) 225 mannitol, 75 sucrose, 1 EGTA, and 20 HEPES-KOH (pH 7.4) with a protease inhibitor cocktail (Complete Mini, Roche Molecular Biochemicals, Mannheim, Germany). Minced samples were homogenized using a Polyton PT-MR3100 (Kinematica, Littau, Switzerland). The homogenate was centrifuged at 13,000 *g* for 15 min, and the supernatant was stored at −80°C until immunoblot analyses. Aliquots of 30 μg protein/lane for each sample were electrophoresed in 12.5% SDS-polyacrylamide gels and electroblotted onto polyvinylidene difluoride membranes (Cosmo Bio, Tokyo, Japan). After being blocked with Tris buffer containing 5% skimmed milk and 0.1% Tween 20, membranes were incubated with antibodies against KChIP2 (Santa Cruz Biotechnology, Santa Cruz, CA) and Kv4.2 (Cell Signaling Technology, Danvers, MA). The anti-Kv4.2 antibody was selected on the basis of results of pilot experiments in which five commercially available antibodies against Kv4.2 were tested. Membranes were then used for reblotting with anti-vinculin antibodies (Sigma-Aldrich, St. Louis, MO) after being stripped using Restore Plus Western Blot Stripping Buffer (Thermo

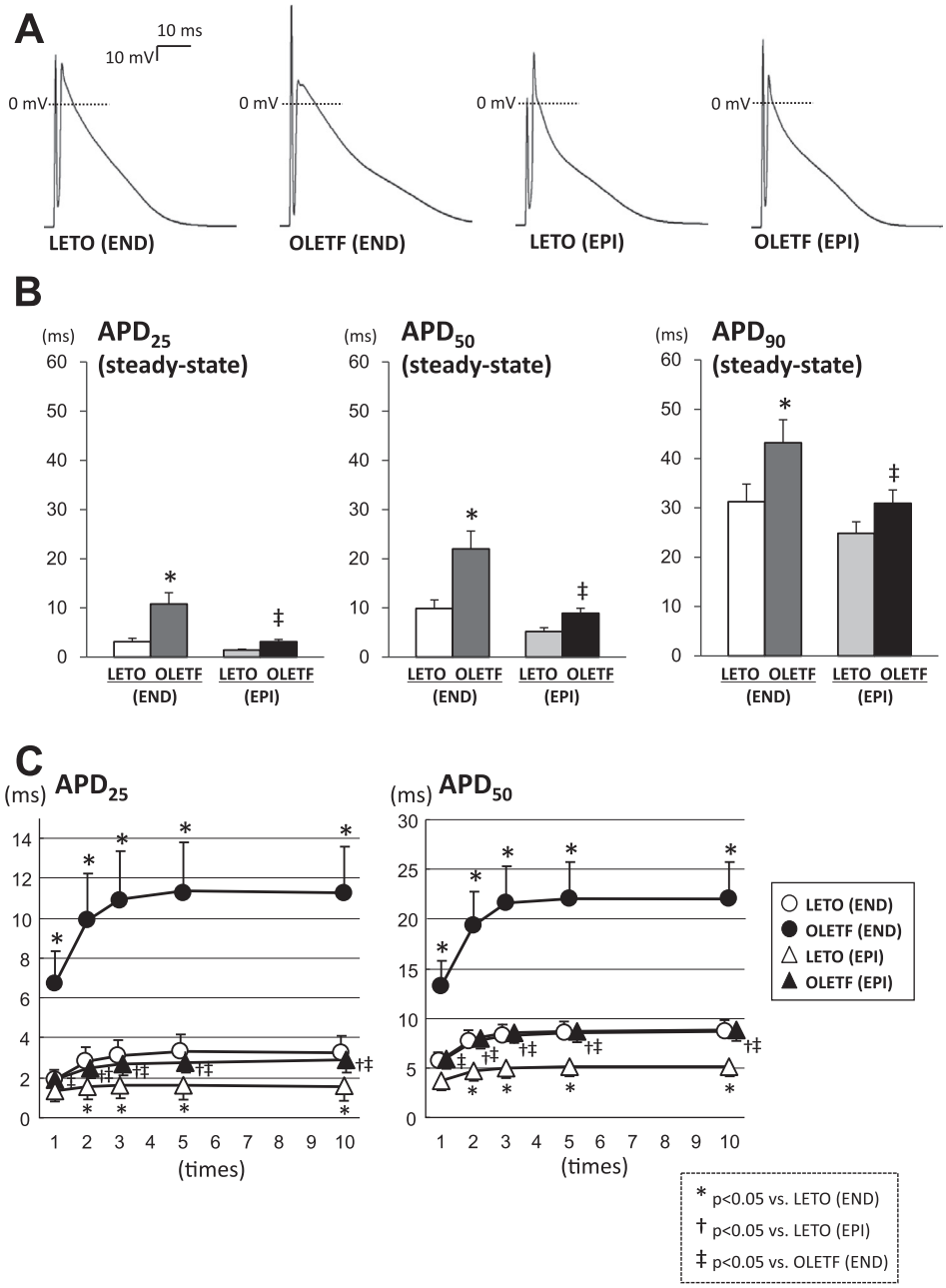

Fig. 1. Action potentials (APs) in subendocardial (Endo) and subepicardial (Epi) myocytes. *A*: representative steady-state AP recordings with stimulation at 1 Hz in myocytes. *B*: comparisons of AP durations (APDs) at 25%, 50%, and 90% repolarization (APD_{25}, APD_{50}, and APD_{90}, respectively) in myocytes between Otsuka-Long-Evans-Tokushima (LETO) and Otsuka-Long-Evans-Tokushima Fatty (OLETF) rats. *C*: relationships between the number of stimulations and APD (APD_{25} and APD_{50}). *n* 21 LETO Endo myocytes, 19 OLETF Endo myocytes, 21 LETO Epi myocytes, and 17 OLETF Epi myocytes. *$P < 0.05$ vs. LETO Endo myocytes; †$P < 0.05$ vs. LETO Epi myocytes; ‡$P < 0.05$ vs. OLETF Endo myocytes.

Scientific, Rockford, IL). Vinculin was used as a loading control. Immunoblotted proteins were visualized using an Immobilon Western detection kit (Millipore, Billerica, MA) and quantified by a luminoimage analyzer (LAS-3000mini, Fujifilm, Tokyo, Japan).

Surface ECG. Under anesthesia by the methods described above, the lead II ECG in OLETF and LETO rats was recorded by a PoweLab data-acquisition system (AD Instruments, Dunedin, New Zealand), and the data were analyzed using LabChart (AD Instru-

Table 1. *Properties of action potentials*

	Subendocardium		Subepicardium	
	LETO rats	OLETF rats	LETO rats	OLETF rats
Number	21	19	21	17
Membrane capacitance, pF	263.0 ± 16.3	252.4 ± 13.0	261.8 ± 12.4	267.3 ± 15.3
Resting membrane potential, mV	−83.8 ± 0.30	−83.5 ± 0.24	−83.3 ± 0.23	−83.9 ± 0.25
Overshoot, mV	24.2 ± 2.48	14.2 ± 1.56*	21.6 ± 1.86	12.1 ± 1.53†
dV/dt_{max}, V/s	195.6 ± 15.8	94.0 ± 10.5*	184.2 ± 13.0	120.1 ± 9.7†

Values are presented as means ± SE. LETO rats, Otsuka-Long-Evans-Tokushima rats; OLETF rats, Otsuka-Long-Evans-Tokushima Fatty rats; dV/dt_{max}, maximum rate of depolarization. *$P < 0.05$ vs. LETO subendocardium; †$P < 0.05$ vs. LETO subepicardium.

ments). Intervals and amplitudes in the ECG were determined for 10 heartbeats and averaged in each animal.

Statistical analysis. All data are expressed as means ± SE. Since data were collected from two regions (the Endo and Epi) in two rat groups (OLETF and LETO), differences between data were tested by two-way ANOVA, but two-way repeated-measures ANOVA was used for testing differences in APD data from repetitive stimulation. The Student-Newman-Keuls post hoc test was used for multiple comparisons when ANOVA indicated significant differences. In all tests, differences were considered to be statistically significant if P values were <0.05.

RESULTS

Body weights and plasma glucose levels. OLETF rats had significantly larger body weights than LETO rats (649.3 ± 7.7 vs. 549.3 ± 9.0 g, $P < 0.05$). The plasma glucose level was significantly higher in OLETF rats than in LETO rats (286.4 ± 10.5 vs. 118.2 ± 4.2 mg/dl, $P < 0.05$), confirming an obese T2DM phenotype in OLETF rats. The results were consistent with the results of our previous studies (7, 17, 35) showing hyperinsulinemia, insulin resistance, and hypertriglyceridemia in OLETF rats at the same age.

Characteristics of APs. Steady-state APD_{25}, APD_{50}, and APD_{90} at 1-Hz stimulation were significantly prolonged in Endo myocytes of OLETF rats compared with Endo myocytes of LETO rats and compared with Epi myocytes of OLETF rats (Fig. 1, *A* and *B*). Although APDs in Epi myocytes tended to be longer in OLETF rats than in LETO rats, the difference did not reach statistical significance (Fig. 1, *A* and *B*). Figure 1*C* shows the relationship between APD and the number of electrical stimulations at 1 Hz. APD was prolonged and differences between APDs in OLETF and LETO rats became larger after repetitive stimulations until they reached a plateau at the 5th stimulation. APD_{25} and APD_{50} in both Endo and Epi myocytes were significantly prolonged in OLETF rats compared with those in LETO rats at all numbers of stimulations except for APD_{25} in Epi myocytes at the 1st stimulation (Fig. 1*C*). There was no significant difference in membrane capacitance or resting membrane potential between LETO and OLETF rats. However, overshoot and dV/dt_{max} were significantly reduced in both Endo and Epi myocytes in OLETF rats compared with those in LETO rats (Table 1).

Ion current densities. As shown in Fig. 2, steady-state I_{to} density ($I_{peak} - I_{ss}$) evoked at 0.1 Hz was larger in Epi myocytes than in Endo myocytes. There was a significant reduction in steady-state I_{to} density in Endo myocytes of OLETF rats compared with that in Endo myocytes of LETO

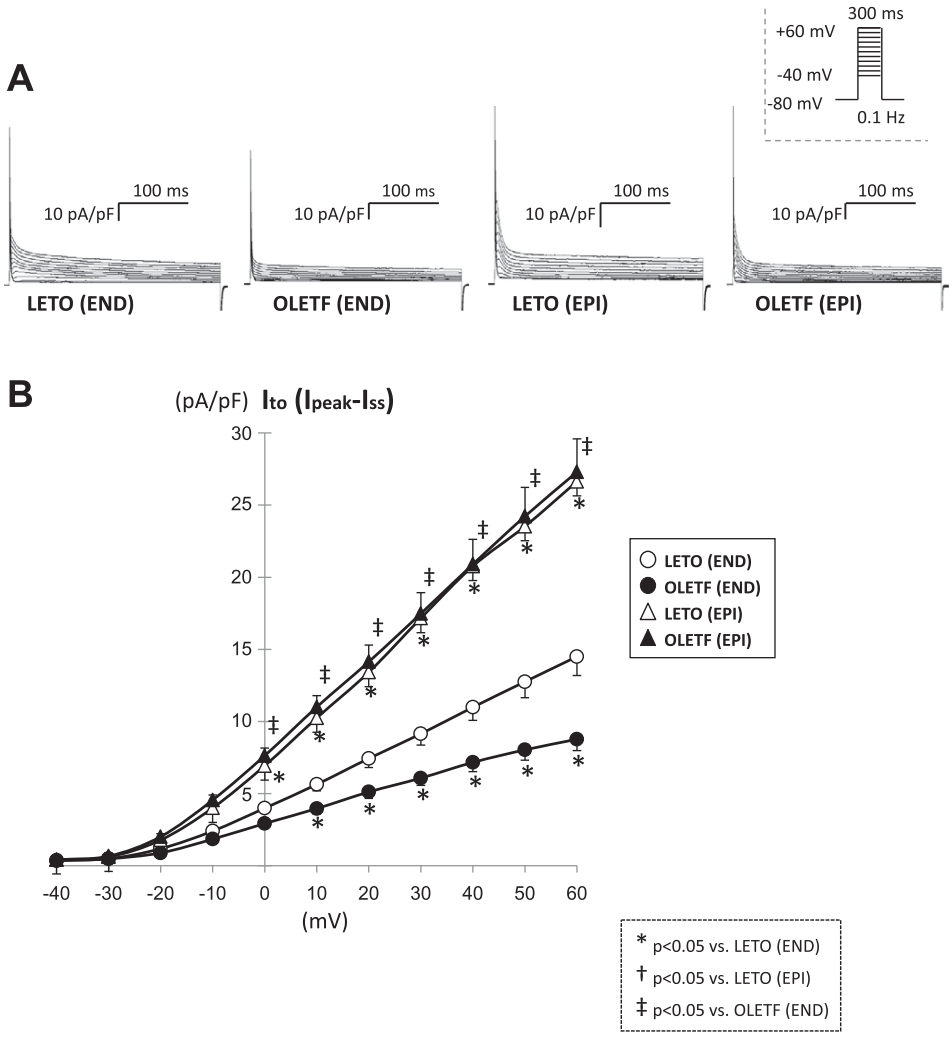

Fig. 2. Density of transient outward K^+ (I_{to}) current [peak current (I_{peak}) − sustained outward current (I_{ss})] in isolated myocytes. *A*: representative steady-state I_{to} current recordings defined as $I_{peak} - I_{ss}$ with stimulation at 0.1 Hz in myocytes. *Inset*: the recording protocol in measurements of steady-state I_{to} densities. *B*: current-voltage relationships of I_{to} in myocytes. $n = 16$ LETO Endo myocytes, 12 OLETF Endo myocytes, 16 LETO Epi myocytes, and 13 OLETF Epi myocytes. *$P <$ 0.05 vs. LETO Endo myocytes; †$P < 0.05$ vs. LETO Epi myocytes; ‡$P < 0.05$ vs. OLETF Endo myocytes.

rats, whereas a statistically significant difference was not observed in Epi myocytes (Fig. 2*B*). To eliminate capacitative artifacts, we also measured I_{to} as a current sensitive to a high concentration (3 mM) of 4-AP (Fig. 3). Consistent with the current of $I_{peak} - I_{ss}$, the 3 mM 4-AP-sensitive current in OLETF rats was significantly smaller than that in LETO rats in Endo myocytes but not in Epi myocytes. In contrast to the results obtained with 3 mM, there was no difference in the current sensitive to 50 μM 4-AP between OLETF and LETO rats in either Endo myocytes (LETO rats: 1.45 ± 0.26 pA/pF, $n = 12$; OLETF rats: 1.28 ± 0.27 pA/pF, $n = 9$, at +20 mV) or Epi myocytes (LETO rats: 2.28 ± 0.26 pA/pF, $n = 12$; OLETF rats: 2.19 ± 0.38 pA/pF, $n = 11$, at +20mV).

As in previous studies using rats, including ours (14, 20), the negative slope within the approximately −50- to −40-mV range in the voltage-I_{K1} relationship was very slight in LETO and OLETF rats, and there was no intergroup difference in I_{K1} density (Fig. 4). A persistent reduction of $I_{Ca,L}$ density was not observed in Epi myocytes of OLETF rats compared with LETO rats. There was also no significantly difference in $I_{Ca,L}$ density in Endo myocytes between OLETF and LETO rats, although slight differences were observed between $I_{Ca,L}$ densities at approximately −20 to −30 mV in Epi myocytes between the two groups and in Endo and Epi myocytes of OLETF rats (Fig. 5*B*).

Recovery of I_{to} from inactivation. As shown in Table 2 and Fig. 6, the contribution of the fast recovering component of I_{to} in both Endo and Epi myocytes was significantly reduced in OLETF rats compared with LETO rats. However, there was no statistically significant difference in the time constants of the fast or slow component of I_{to} between the two groups.

Expression of mRNA and proteins regulating ion current. As shown in Fig. 7, quantitative RT-PCR showed that the mRNA level of *KCND2*, a gene coding for Kv4.2 (a pore-forming subunit of I_{to}), in Endo myocytes was significantly lower in OLETF rats than in LETO rats, although the difference in Epi

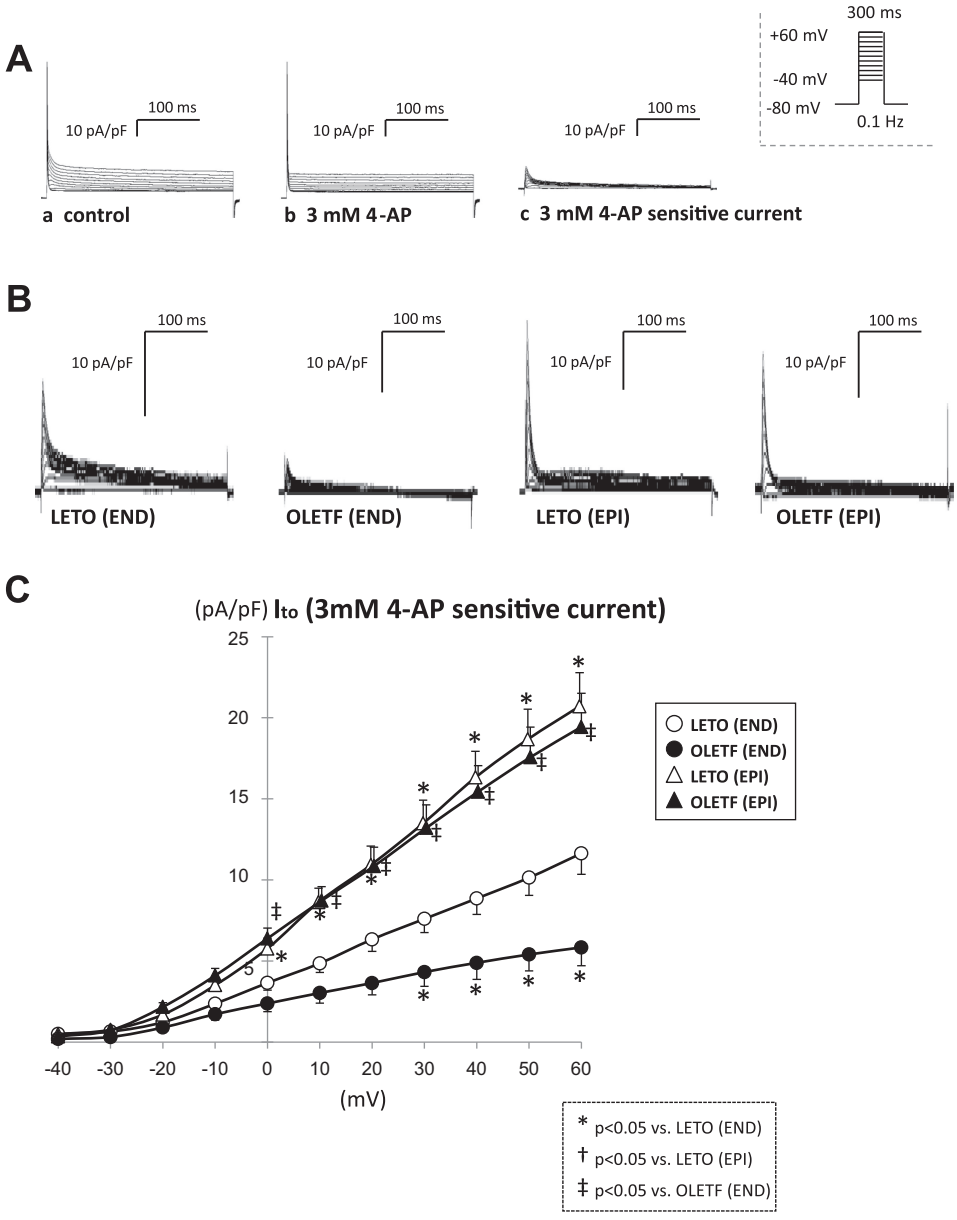

Fig. 3. Density of I_{to} [3 mM 4-aminopyridine (4-AP)-sensitive current] in isolated myocytes. From control outward currents (*A*,*a*), currents resistant to 3 mM 4-AP (*A*,*b*) were subtracted, yielding the 3 mM 4-AP-sensitive current (*A*,*c*). *Inset*: the recording protocol in measurements of 3 mM 4-AP-sensitive currents. *B*: representative 3 mM 4-AP-sensitive current recordings with stimulation at 0.1 Hz in myocytes. *C*: current-voltage relationships of 3 mM 4-AP-sensitive currents. $n = 10$ LETO Endo myocytes, 9 OLETF Endo myocytes, 10 LETO Epi myocytes, and 11 OLETF Epi myocytes. *$P < 0.05$ vs. LETO Endo myocytes; ‡$P < 0.05$ vs. OLETF Endo myocytes.

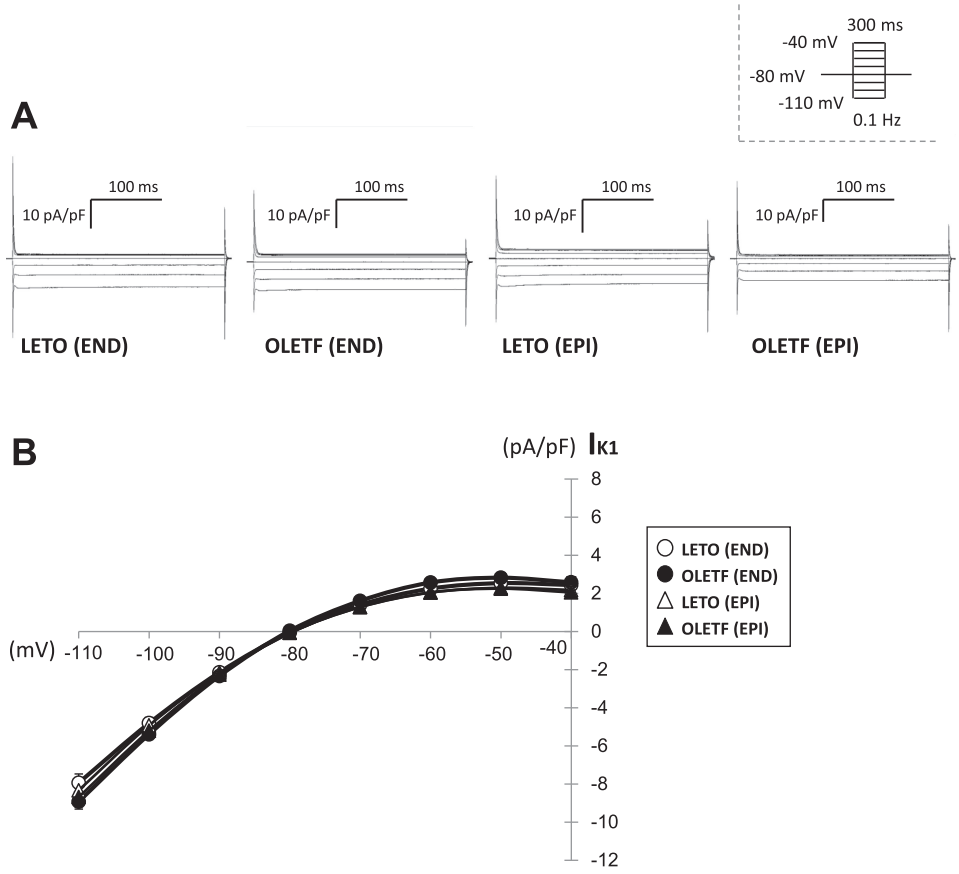

Fig. 4. Inward rectifier K^+ current (I_{K1}) density in isolated myocytes. *A*: representative steady-state I_{K1} recordings with stimulation at 0.1 Hz in myocytes. *Inset*: the recording protocol in measurements of steady-state I_{K1} densities. *B*: current-voltage relationships of I_{K1}. n = 15 LETO Endo myocytes, 14 OLETF Endo myocytes, 17 LETO Epi myocytes, and 14 OLETF Epi myocytes.

myocytes was statistically insignificant. mRNA levels of other pore-forming subunits of I_{to}, Kv4.3 and Kv1.4, were similar in OLETF and LETO rats. The mRNA level of I_{to} channel accessory subunit KChIP2 (*KCNIP2*) was significantly lower in Endo myocytes of OLETF rats than those of LETO rats, although its levels in Epi myocytes were similar in OLETF and LETO rats. There was no significant intergroup difference between OLETF and LETO rats in mRNA levels of MiRP3, which is also a possible I_{to} β-subunit regulating Kv4.2 in a KChIP-dependent manner (13). mRNA levels of Nav1.5 (*SCN5A*), a Na^+ channel-forming protein, were also comparable in OLETF and LETO rats.

The Kv4.2 protein level in Endo myocytes was significantly lower in OLETF rats than in LETO rats, although Kv4.2 levels in Epi myocytes were comparable in the two groups (Fig. 8*A*). These results were consistent with differences in Kv4.2 mRNA levels between OLETF and LETO rats in Endo myocytes (Fig. 7, *top left*). In contrast to the Kv4.2 level, the KChIP2 protein level was significantly reduced not only in Endo but also in Epi myocytes in OLETF rats compared with those in LETO rats (Fig. 8*B*).

Gene expression of Irx5. Recent studies (3, 6) have shown that the transcription factor Irx5 negatively regulates Kv4.2 with the coexistence of Irx4 and that gene expression of Irx5 in Endo myocytes is higher than that in Epi myocytes, leading to the formation of a physiological transmural gradient of I_{to}. Therefore, we determined whether alterations in Irx5 and Irx4 gene expression are responsible for region-specific alterations of I_{to} and Kv4.2 expression in OLETF rats. As shown in Fig. 9, Irx5 mRNA was almost exclusively expressed in Endo myocytes, and its level was significantly higher in OLETF rats than in LETO rats. In contrast, mRNA levels of Irx4 were comparable in Endo and Epi myocytes, and levels were similar in OLETF and LETO rats (Fig. 9).

Surface ECG. Heart rate was significantly lower in OLETF rats than in LETO rats (310 ± 9 vs. 383 ± 5 beats/min, n = 3 each). However, there were no significant differences between the two groups in the PR interval (46.5 ± 3.2 vs. 40.1 ± 1.6 ms), QRS interval (15.0 ± 1.0 vs. 19.1 ± 2.2 ms), QT interval (63.8 ± 4.2 vs. 84.7 ± 9.9 ms), interval from the Q wave to the peak of the T wave (24.5 ± 0.5 vs. 30.8 ± 4.0 ms), interval from the Q wave to the end of the T wave (63.8 ± 4.2 vs. 84.7 ± 9.9 ms), R amplitude (566.3 ± 98.0 vs. 494.1 ± 29.6 μV), or T amplitude (90.2 ± 7.6 vs. 85.3 ± 20.2 μV).

DISCUSSION

The present study showed the transmural difference in APD modification associated with T2DM. Steady-state APD (i.e., APD at the 15th stimulation) in Endo myocytes evoked by stimulation at 1 Hz was significantly longer in OLETF rats than in LETO rats. APDs during repetitive stimulation in both Endo and Epi myocytes were significantly more prolonged in OLETF rats than in LETO rats, although the difference between the two groups was larger in Endo myocytes (Fig. 1). A plausible explanation for the Endo-predominant APD prolongation in OLETF rats is transmural heterogeneity of current modification. $I_{Ca,L}$ and I_{K1} were similar in OLETF and LETO

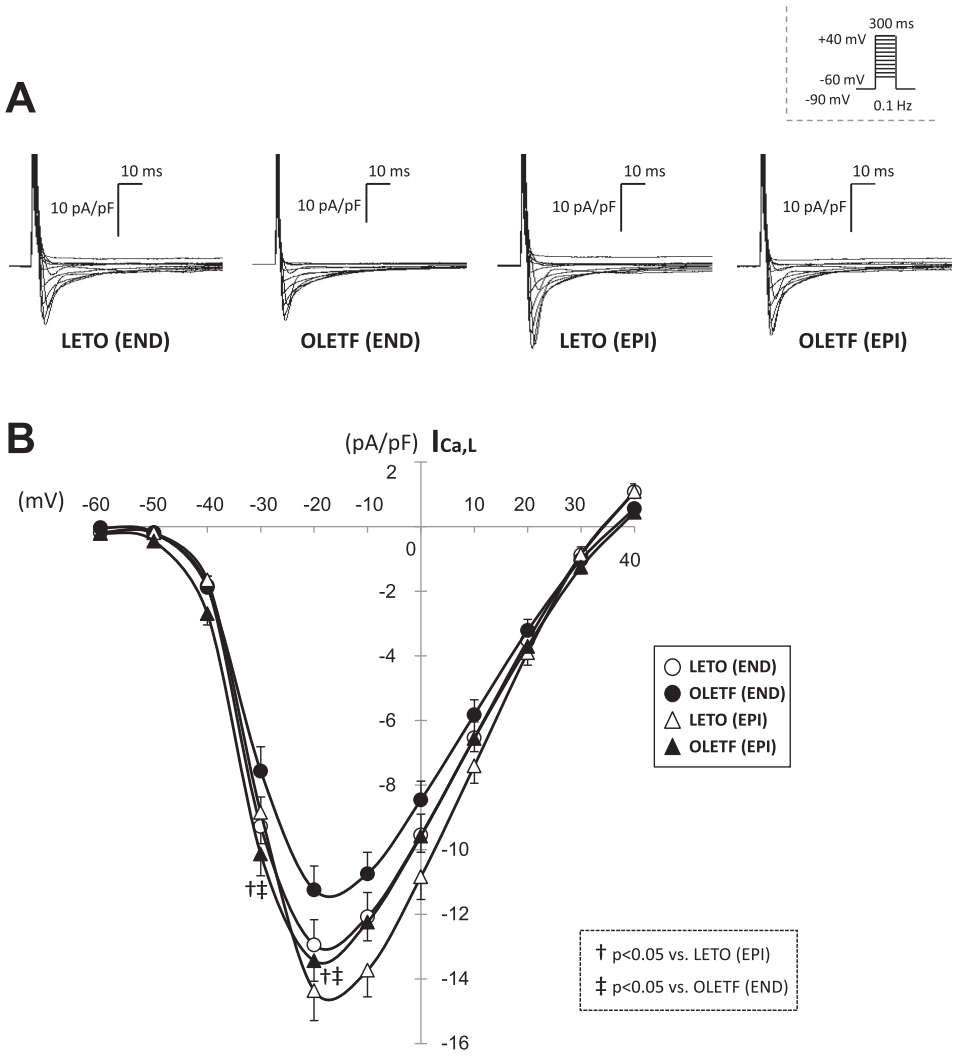

Fig. 5. L-type Ca^{2+} current ($I_{Ca,L}$) density in isolated myocytes. *A*: representative steady-state $I_{Ca,L}$ recordings with stimulation at 0.1 Hz in myocytes. *Inset*: the recording protocol in measurements of steady-state $I_{Ca,L}$ densities. *B*: current-voltage relationships of $I_{Ca,L}$. $n = 20$ LETO Endo myocytes, 20 OLETF Endo myocytes, 20 LETO Epi myocytes, and 20 OLETF Epi myocytes. †$P < 0.05$ vs. LETO Epi myocytes; ‡$P < 0.05$ vs. OLETF Endo myocytes.

rats. However, the slope of the current-voltage relationship of I_{to} was smaller in Endo myocytes from OLETF rats than in those from LETO rats, although the difference in the current density of I_{to} at 0 mV was small (Figs. 2 and 3). In contrast, such a difference in the current-voltage relationship was not observed for I_{to} in Epi myocytes. Interestingly, the relative proportion of the fast recovering component of I_{to} inactivation in OLETF rats was reduced compared with that in LETO rats, and the reduction in the fast component of I_{to} recovery was larger in Endo myocytes than in Epi myocytes (Table 2 and Fig. 6). These findings are consistent with stronger rate dependence of the APD in Endo myocytes of OLETF rats (Fig. 1*C*). Collectively, the results suggest that APD in OLETF rats is prolonged in Endo myocytes with two mechanisms, a reduction in the current density of I_{to} and a reduction in the fast recovering component of I_{to}, being involved in contrast to Epi myocytes, in which the change in the fast recovering component of I_{to} is the only factor leading to a trend for prolongation of APD.

In addition to the modification of I_{to}, a reduction in I_{Na} might have been involved in APD prolongation in OLETF rats. The AP overshoot and dV/dt_{max} were reduced (Table 1) and expression of KChIP2, which potentially augments I_{Na} (33), was reduced in OLETF rats. Decreased I_{Na} could reduce the peak of AP, which would, in turn, potentially reduce the number of K^+ channels activated, leading to APD prolongation.

Consistent with regionally different modification of I_{to} in OLETF rats, corresponding downregulation was observed for Kv4.2 and KChIP2 (Fig. 8). KChIP2 modulates the function of Kv channels by modifying trafficking of Kv channel proteins and the kinetics of inactivation and also by acceleration of the kinetics from recovery from inactivation (1, 12, 15, 23). Although specific effects of KChIP2 deletion on the fast and slow components of I_{to} recovery have not been systematically examined, a previous study (12) showed that the effect of a lack of KChIP2 on the fast component of recovery of I_{to} was more predominant than that on the slow component. A modest delay in recovery from inactivation was the only change in I_{to} in Epi myocytes of OLETF rats, in which expression of KChIP2, but not that of Kv4.2, was reduced. mRNA levels of Kv4.3 and Kv1.4 in Epi and Endo myocytes were comparable in LETO and OLETF rats (Fig. 8) (41). The lack of difference in Kv1.4 mRNA levels between OLETF and LETO rats was consistent with the present results showing that current sensitive to 50 μM 4-AP, which represents the component with slow inactivation kinetics via Kv1.4 (43, 47), was similar in OLETF and

Table 2. *Gating parameters of recovery from inactivation of cardiomyocytes*

	Subendocardium		Subepicardium	
	LETO rats	OLETF rats	LETO rats	OLETF rats
Number	5	8	7	7
τ_{fast}, ms	7.02 ± 0.44	5.50 ± 0.58	4.82 ± 0.20	5.39 ± 0.80
τ_{slow}, ms	4293 ± 1685	1574 ± 354	2340 ± 627	2126 ± 626
A_{fast}	0.871 ± 0.039	0.618 ± 0.035*	0.957 ± 0.013	0.883 ± 0.029†
A_{slow}	0.129 ± 0.039	0.382 ± 0.035	0.043 ± 0.013	0.117 ± 0.029

Values are presented as means ± SE. τ_{fast} and τ_{slow}, time constants for recovery of the fast and slow components, respectively; A_{fast} and A_{slow}, contributions of the fast and slow components to recovery, respectively. *$P < 0.05$ vs. LETO subendocardium; †$P < 0.05$ vs. LETO subepicardium.

LETO rats. Taken together, the present results support the notion that downregulation of Kv4.2 protein expression contributes to the reduced I_{to} density in Endo myocytes, whereas downregulation of KChIP2 expression underlies the reduction in the fast recovering component of I_{to} from inactivation in both Endo and Epi myocytes in OLETF rats.

The KChIP2 protein level was decreased in both Endo and Epi myocytes, whereas its mRNA level was decreased only in Endo myocytes of OLETF rats. A similar discrepancy between KChIP2 protein and mRNA levels has been reported for peroxisome proliferator-activated receptor-α-overexpressed metabolic cardiomyopathy (16). A plausible explanation for the present data on KChIP2 protein and mRNA levels is increased degradation of KChIP2 protein or suppressed translation of KChIP2 in Epi myocytes.

Using Irx5-deficient mice, Costantini et al. (3) first demonstrated that Irx5 played an important role in the formation of a physiological transmural gradient of APD by negatively regulating Kv4.2. Recent studies (4, 26, 34) have shown that in other species, including rats, dogs, and humans, Irx5 is ex-

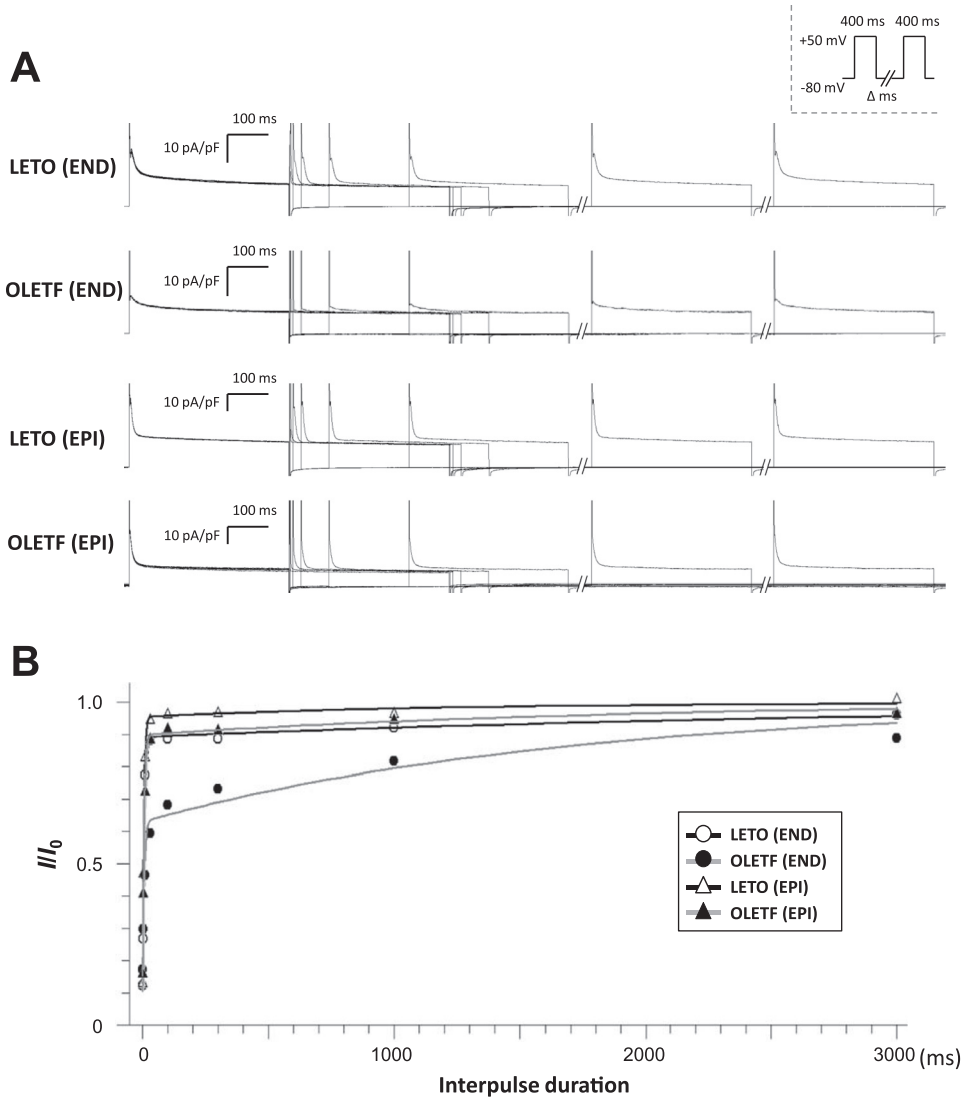

Fig. 6. Recovery of I_{to} from inactivation. *A*: representative results of experiments for determining the recovery of I_{to} ($I_{peak} - I_{ss}$) from inactivation in myocytes at interpulse durations of 1, 3, 10, 30, 100, 300, 1,000, and 3,000 ms. *Inset*: the double-pulse protocol in measurements of recovery from inactivation of I_{to}. *B*: relationships between the interval of two identical depolarizing pulses and the rate of recovery in myocytes. Data on relative currents were fitted using the following two-exponential function: $I/I_0 = 1 - A_{fast}\exp(-t/\tau_{fast}) - A_{slow}\exp(-t/\tau_{slow})$, $A_{fast} + A_{slow} = 1$, where A_{fast} and A_{slow} are contributions of the fast and slow components to recovery, respectively, t is time, and τ_{fast} and τ_{slow} are the time constants for recovery of the fast and slow components, respectively. $n = 5$ LETO Endo myocytes, 8 OLETF Endo myocytes, 7 LETO Epi myocytes, and 7 OLETF Epi myocytes.

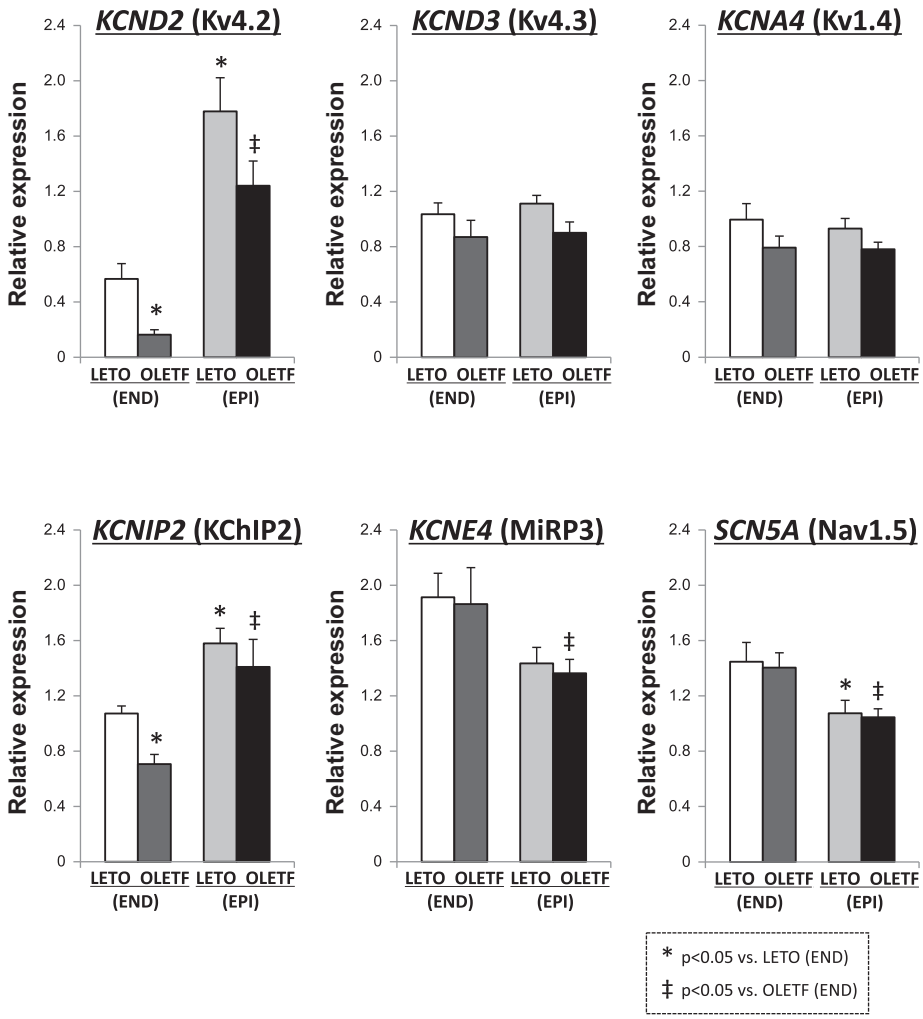

Fig. 7. mRNA levels of channel subunits regulating K^+ and Na^+ currents. mRNA levels of genes coding K^+ channel pore proteins (Kv4.2, Kv4.3, and Kv1.4), genes coding regulatory subunits [voltage-gated K^+ channel-interacting protein 2 (KChIP2) and MiRP3], and a gene coding Na^+ channel pore protein (Nav.1.5) were determined by quantitative RT-PCR and are shown for the Endo and Epi in LETO and OLETF rats. $n = 6$ LETO Endo myocytes, 6 OLETF Endo myocytes, 6 LETO Epi myocytes, and 6 OLETF EPI myocytes. *$P < 0.05$ vs. LETO Endo myocytes; ‡$P < 0.05$ vs. OLETF Endo myocytes.

pressed at a higher level in Endo myocytes than in Epi myocytes, being consistent with an inverse gradient of Kv4.2 expression. We confirmed Endo-dominant Irx5 expression and found that Irx5 expression was upregulated by T2DM selectively in Endo myocytes (Fig. 9). The mechanism of upregulation of Irx5 in OLETF rats remains unclear, although downregulation of microRNA-1 (mir-1), which negatively regulates Irx5 (8, 46), is a possibility.

Previous studies (31, 38, 45) have consistently shown that steady-state I_{to} density and the fast component of I_{to} recovery are reduced in animal models of T1DM. As for heterogeneity of the impact of T1DM on I_{to}, Shimoni et al. (31) showed that the difference in I_{to} between streptozotocin-induced diabetic rats and nondiabetic control rats was larger in Epi than in Endo myocytes. However, different changes in I_{to} have been reported in animal models of T2DM [no change in fructose-fed rats (30) and a significant reduction in male *ob*/*ob* mice (29)], and the transmural heterogeneity in the effect of T2DM ion currents has not been examined. The present study showed, for the first time, an Endo-specific reduction in I_{to} density and an Endo-predominant reduction in the fast component of I_{to} recovery from inactivation. Collectively, the findings indicate that T1DM and T2DM have distinct impacts on I_{to} and that hyperglycemia is not sufficient for the reduction of I_{to} and downregulation of channel expression.

Recent studies (10, 22) have shown that MAPK and NF-κB are involved in the downregulation of KChIP2 gene expression in the hypertrophied myocardium. However, data on membrane capacitance (Table 1) and data on cross-sectional areas of the myocyte (data not shown) indicate that there was no significant myocyte hypertrophy in either the Endo or Epi of OLETF rats at 25–30 wk of age. MAPK phosphorylation levels in the myocardium were comparable in OLETF and LETO rats in our previous study (17), and the level of translocation of p65, a marker for NF-κB activation, to nuclei was not enhanced in OLETF (data not shown). Thus, different molecular mechanisms are likely to be involved in the downregulation of KChIP2 expression in T2DM hearts and that in hypertrophied hearts.

In contrast to the marked differences in APDs and I_{to} between OLETF and LETO rats, surface ECGs were similar in the two groups. Since Weber dos Santos et al. (39) reported that a blocker of I_{to}, 4-AP, shifted the peak of T wave to the right in ECGs, we expected that the interval from the Q wave to the peak of the T wave would be longer in OLETF rats. However, that was not the case. The reason for the lack of differences in the surface ECG between OLETF and LETO rats is unclear, but a few explanations are possible. First, APD changes in Epi myocytes have a greater impact on T wave morphology and QT interval than do those in Endo myocytes

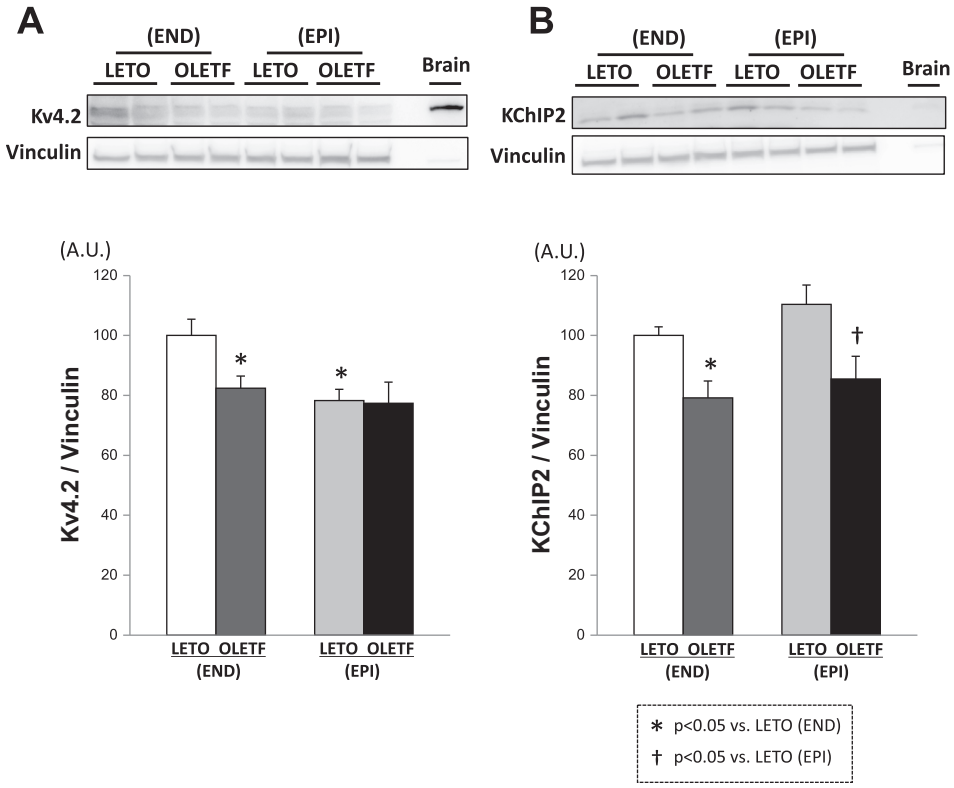

Fig. 8. Protein levels of I_{to} channel subunits. *Top*: representative immunoblots for Kv4.2 and KChIP2 with those for a loading control (vinculin). *Bottom*: group mean data on these proteins. $n = 7$ for Kv4.2 and 7 for KChIP2. *$P < 0.05$ vs. LETO Endo myocytes; †$P < 0.05$ vs. LETO Epi myocytes.

(39). Thus, the Endo-predominant change in OLETF rats might not have been large enough to be detected by the surface ECG. Second, there are not only transmural but also apex-to-base gradients in APD in rat hearts, which also could have masked changes in Endo myocytes (39). Third, unlike APDs in isolated myocytes, the ECG from hearts in situ is under the influence of the autonomic nervous system.

ECG changes in diabetic patients include QT prolongation and increased QT dispersion (5, 21, 40). QT dispersion is more strongly associated with cardiovascular events than is QT prolongation in diabetic patients. Possible factors underlying the diabetes-associated changes in ECG are autonomic neuropathy, perfusion abnormalities, and modified ion channel expression. Unfortunately, information regarding disease-induced ion channel expression in human hearts is very limited, and the results of studies regarding changes in KChIP2 expression and Kv4.3 expression in heart failure patients are discrepant (24, 32, 48). The present findings in OLETF rats indicate the possibility that special heterogeneity in the impact of T2DM on ion currents and expression of channel proteins underlie the QT dispersion of human diabetic hearts, although such channel remodeling precedes the manifestation of ECG changes by diabetes.

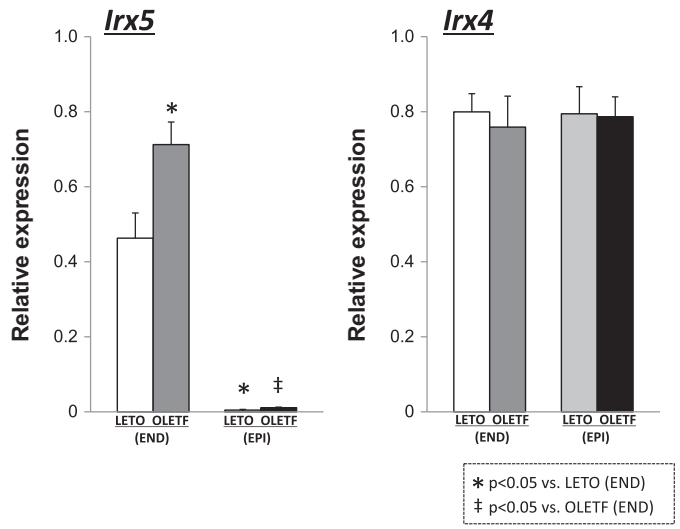

Fig. 9. mRNA levels of Iroquois homeobox 4 and 5 (Irx5 and Irx4, respectively). mRNA levels of Irx5 and Irx4 were determined by quantitative RT-PCR in the ventricular Endo and Epi in LETO and OLETF rats. $n = 6$ for the LETO Endo, 6 for the OLETF Endo, 6 for the LETO Epi, and 6 for the OLETF Epi. *$P < 0.05$ vs. the LETO Endo; ‡$P < 0.05$ vs. the OLETF Endo.

There are limitations in this study. The present observations regarding APD and I_{to} may not be generalized in all stages of T2DM and in all types of T2DM. Second, since we used a rat model of T2DM, it was not possible to evaluate the impact of T2DM on delayed rectifier K^+ currents (rapid and slow components of the delayed rectifier K^+ current), which underlie the late phase of the AP in large animals, including humans. Xiao et al. (42) reported that *KCNH2*, which encodes rapid component of delayed rectifier K^+ channels, was repressed via upregulation of microRNA-133 in a rabbit model of T1DM. Whether similar modification of delayed rectifier K^+ currents is induced by T2DM remains unclear, and animal models of T2DM other than rats and mice are necessary to address this issue.

In conclusion, T2DM induces Endo-predominant APD prolongation in which a reduced fast component of I_{to} recovery from inactivation and reduced steady-state I_{to} by downregulation of Kv4.2 and KChIP2 expression are involved. Upregula-

tion of Irx5 in the Endo may contribute to the Kv4.2 down-regulation in T2DM.

GRANTS

This work was supported in part by Japan Society for the Promotion of Science Grant-In-Aid for Young Scientists (B) 24790218.

DISCLOSURES

No conflicts of interest, financial or otherwise, are declared by the author(s).

AUTHOR CONTRIBUTIONS

Author contributions: T.S., T. Miura, and N.T. conception and design of research; T.S., S.I., and T. Kojima performed experiments; T.S., T. Kobayashi, A.K., T. Miki, M.T., H.K., T.I., S.I., T. Kojima, T. Miura, and N.T. analyzed data; T.S., T. Kobayashi, A.K., T. Miki, M.T., H.K., T.I., S.I., T. Kojima, T. Miura, and N.T. interpreted results of experiments; T.S. and T. Kojima prepared figures; T.S., A.K., T. Miki, and M.T. drafted manuscript; T.S., T. Kobayashi, A.K., T. Miki, M.T., H.K., T.I., S.I., T. Kojima, T. Miura, and N.T. approved final version of manuscript; T. Kobayashi, A.K., M.T., T. Kojima, T. Miura, and N.T. edited and revised manuscript.

REFERENCES

1. **An WF, Bowlby MR, Betty M, Cao J, Ling HP, Mendoza G, Hinson JW, Mattsson KI, Strassle BW, Trimmer JS, Rhodes KJ.** Modulation of A-type potassium channels by a family of calcium sensors. *Nature* 403: 553–556, 2000.
2. **Boudina S, Abel ED.** Diabetic cardiomyopathy revisited. *Circulation* 115: 3213–3223, 2007.
3. **Costantini DL, Arruda EP, Agarwal P, Kim KH, Zhu Y, Zhu W, Lebel M, Cheng CW, Park CY, Pierce SA, Guerchicoff A, Pollevick GD, Chan TY, Kabir MG, Cheng SH, Husain M, Antzelevitch C, Srivastava D, Gross GJ, Hui CC, Backx PH, Bruneau BG.** The homeodomain transcription factor Irx5 establishes the mouse cardiac ventricular repolarization gradient. *Cell* 123: 347–358, 2005.
4. **Gaborit N, Varro A, Le Bouter S, Szuts V, Escande D, Nattel S, Demolombe S.** Gender-related differences in ion-channel and transporter subunit expression in non-diseased human hearts. *J Mol Cell Cardiol* 49: 639–646, 2010.
5. **Giunti S, Gruden G, Fornengo P, Barutta F, Amione C, Ghezzo G, Cavallo-Perin P, Bruno G.** Increased QT interval dispersion predicts 15-year cardiovascular mortality in type 2 diabetic subjects: the population-based Casale Monferrato Study. *Diabetes Care* 35: 581–583, 2012.
6. **He W, Jia Y, Takimoto K.** Interaction between transcription factors Iroquois proteins 4 and 5 controls cardiac potassium channel Kv4.2 gene transcription. *Cardiovasc Res* 81: 64–71, 2009.
7. **Hotta H, Miura T, Miki T, Togashi N, Maeda T, Kim SJ, Tanno M, Yano T, Kuno A, Itoh T, Satoh T, Terashima Y, Ishikawa S, Shimamoto K.** Angiotensin II type 1 receptor-mediated upregulation of calcineurin activity underlies impairment of cardioprotective signaling in diabetic hearts. *Circ Res* 106: 129–132, 2010.
8. **Ikeda S, Kong SW, Lu J, Bisping E, Zhang H, Allen PD, Golub TR, Pieske B, Pu WT.** Altered microRNA expression in human heart disease. *Physiol Genomics* 31: 367–373, 2007.
9. **Ishikawa S, Kuno A, Tanno M, Miki T, Kouzu H, Itoh T, Sato T, Sunaga D, Murase H, Miura T.** Role of connexin-43 in protective PI3K-Akt-GSK-3β signaling in cardiomyocytes. *Am J Physiol Heart Circ Physiol* 302: H2536–H2544, 2012.
10. **Jia Y, Takimoto K.** Mitogen-activated protein kinases control cardiac KChIP2 gene expression. *Circ Res* 98: 386–393, 2006.
11. **Kassiri Z, Hajjar R, Backx PH.** Molecular components of transient outward potassium current in cultured neonatal rat ventricular myocytes. *J Mol Med* 80: 351–358, 2002.
12. **Kobayashi T, Yamada Y, Nagashima M, Seki S, Tsutsuura M, Ito Y, Sakuma I, Hamada H, Abe T, Tohse N.** Contribution of KChIP2 to the developmental increase in transient outward current of rat cardiomyocytes. *J Mol Cell Cardiol* 35: 1073–1082, 2003.
13. **Levy DI, Cepaitis E, Wanderling S, Toth PT, Archer SL, Goldstein SA.** The membrane protein MiRP3 regulates Kv4.2 channels in a KChIP-dependent manner. *J Physiol* 588: 2657–2668, 2010.
14. **Liu QY, Rosen MR, McKinnon D, Robinson RB.** Sympathetic innervation modulates repolarizing K^+ currents in rat epicardial myocytes. *Am J Physiol Heart Circ Physiol* 274: H915–H922, 1998.
15. **Lundby A, Jespersen T, Schmitt N, Grunnet M, Olesen SP, Cordeiro JM, Calloe K.** Effect of the I_{to} activator NS5806 on cloned K_v4 channels depends on the accessory protein KChIP2. *Br J Pharmacol* 160: 2028–2044, 2010.
16. **Marionneau C, Aimond F, Brunet S, Niwa N, Finck B, Kelly DP, Nerbonne JM.** PPARα-mediated remodeling of repolarizing voltage-gated K^+ (K_v) channels in a mouse model of metabolic cardiomyopathy. *J Mol Cell Cardiol* 44: 1002–1015, 2008.
17. **Miki T, Miura T, Hotta H, Tanno M, Yano T, Sato T, Terashima Y, Takada A, Ishikawa S, Shimamoto K.** Endoplasmic reticulum stress in diabetic hearts abolishes erythropoietin-induced myocardial protection by impairment of phospho-glycogen synthase kinase-3β-mediated suppression of mitochondrial permeability transition. *Diabetes* 58: 2863–2872, 2009.
18. **Miki T, Yuda S, Kouzu H, Miura T.** Diabetic cardiomyopathy: pathophysiology and clinical features. *Heart Fail Rev* 18: 149–166, 2013.
19. **Moran TH, Bi S.** Hyperphagia and obesity in OLETF rats lacking CCK-1 receptors. *Philos Trans R Soc Lond Biol Sci* 361: 1211–1218, 2006.
20. **Nagashima M, Tohse N, Kimura K, Yamada Y, Fujii N, Yabu H.** Alternation of inwardly rectifying background K^+ channel during development of rat fetal cardiomyocytes. *J Mol Cell Cardiol* 33: 533–543, 2001.
21. **Okin PM, Devereux RB, Lee ET, Galloway JM, Howard BV.** Electrocardiographic repolarization complexity and abnormality predict all-cause and cardiovascular mortality in diabetes: the strong heart study. *Diabetes* 53: 434–440, 2004.
22. **Panama BK, Latour-Villamil D, Farman GP, Zhao D, Bolz SS, Kirshenbaum LA, Backx PH.** Nuclear factor κB downregulates the transient outward potassium current $I_{to,f}$ through control of KChIP2 expression. *Circ Res* 108: 537–543, 2011.
23. **Patel SP, Campbell DL.** Transient outward potassium current, "I_{to}", phenotypes in the mammalian left ventricle: underlying molecular, cellular and biophysical mechanisms. *J Physiol* 569: 7–39, 2005.
24. **Radicke S, Cotella D, Graf EM, Banse U, Jost N, Varro A, Tseng GN, Ravens U, Wettwer E.** Functional modulation of the transient outward current Ito by KCNE β-subunits and regional distribution in human non-failing and failing hearts. *Cardiovasc Res* 71: 695–703, 2006.
25. **Radovits T, Korkmaz S, Loganathan S, Barnucz E, Bomicke T, Arif R, Karck M, Szabo G.** Comparative investigation of the left ventricular pressure-volume relationship in rat models of type 1 and type 2 diabetes mellitus. *Am J Physiol Heart Circ Physiol* 297: H125–H133, 2009.
26. **Rosati B, Grau F, McKinnon D.** Regional variation in mRNA transcript abundance within the ventricular wall. *J Mol Cell Cardiol* 40: 295–302, 2006.
27. **Schroeder M, Zagoory-Sharon O, Shbiro L, Marco A, Hyun J, Moran TH, Bi S, Weller A.** Development of obesity in the Otsuka Long-Evans Tokushima Fatty rat. *Am J Physiol Regul Integr Comp Physiol* 297: R1749–R1760, 2009.
28. **Shang W, Yasuda K, Takahashi A, Hamasaki A, Takehiro M, Nabe K, Zhou H, Naito R, Fujiwara H, Shimono D, Ueno H, Ikeda H, Toyoda K, Yamada Y, Kurose T.** Effect of high dietary fat on insulin secretion in genetically diabetic Goto-Kakizaki rats. *Pancreas* 25: 393–399, 2002.
29. **Shimoni Y, Chuang M, Abel ED, Severson DL.** Gender-dependent attenuation of cardiac potassium currents in type 2 diabetic *db/db* mice. *J Physiol* 555: 345–354, 2004.
30. **Shimoni Y, Ewart HS, Severson D.** Type I and II models of diabetes produce different modifications of K^+ currents in rat heart: role of insulin. *J Physiol* 507: 485–496, 1998.
31. **Shimoni Y, Severson D, Giles W.** Thyroid status and diabetes modulate regional differences in potassium currents in rat ventricle. *J Physiol* 488: 673–688, 1995.
32. **Soltysinska E, Olesen SP, Christ T, Wettwer E, Varro A, Grunnet M, Jespersen T.** Transmural expression of ion channels and transporters in human nondiseased and end-stage failing hearts. *Pflügers Arch* 459: 11–23, 2009.
33. **Stein AB, Jones TA, Herron TJ, Patel SR, Day SM, Noujaim SF, Milstein ML, Klos M, Furspan PB, Jalife J, Dressler GR.** Loss of H3K4 methylation destabilizes gene expression patterns and physiological functions in adult murine cardiomyocytes. *J Clin Invest* 121: 2641–2650, 2011.
34. **Stones R, Billeter R, Zhang H, Harrison S, White E.** The role of transient outward K^+ current in electrical remodelling induced by voluntary exercise in female rat hearts. *Basic Res Cardiol* 104: 643–652, 2009.

35. **Takada A, Miki T, Kuno A, Kouzu H, Sunaga D, Itoh T, Tanno M, Yano T, Sato T, Ishikawa S, Miura T.** Role of ER stress in ventricular contractile dysfunction in type 2 diabetes. *PLOS ONE* 7: e39893, 2012.
36. **Tohse N.** Calcium-sensitive delayed rectifier potassium current in guinea pig ventricular cells. *Am J Physiol Heart Circ Physiol* 258: H1200–H1207, 1990.
37. **Tohse N, Nakaya H, Hattori Y, Endou M, Kanno M.** Inhibitory effect mediated by α_1-adrenoceptors on transient outward current in isolated rat ventricular cells. *Pflügers Arch* 415: 575–581, 1990.
38. **Wang DW, Kiyosue T, Shigematsu S, Arita M.** Abnormalities of K^+ and Ca^{2+} currents in ventricular myocytes from rats with chronic diabetes. *Am J Physiol Heart Circ Physiol* 269: H1288–H1296, 1995.
39. **Weber dos Santos R, Nygren A, Otaviano Campos F, Koch H, Giles WR.** Experimental and theoretical ventricular electrograms and their relation to electrophysiological gradients in the adult rat heart. *Am J Physiol Heart Circ Physiol* 297: H1521–H1534, 2009.
40. **Whitsel EA, Boyko EJ, Rautaharju PM, Raghunathan TE, Lin D, Pearce RM, Weinmann SA, Siscovick DS.** Electrocardiographic QT interval prolongation and risk of primary cardiac arrest in diabetic patients. *Diabetes Care* 28: 2045–2047, 2005.
41. **Wickenden AD, Jegla TJ, Kaprielian R, Backx PH.** Regional contributions of Kv1.4, Kv4.2, and Kv4.3 to transient outward K^+ current in rat ventricle. *Am J Physiol Heart Circ Physiol* 276: H1599–H1607, 1999.
42. **Xiao J, Luo X, Lin H, Zhang Y, Lu Y, Wang N, Yang B, Wang Z.** MicroRNA miR-133 represses HERG K^+ channel expression contributing to QT prolongation in diabetic hearts. *J Biol Chem* 282: 12363–12367, 2007.
43. **Xu H, Guo W, Nerbonne JM.** Four kinetically distinct depolarization-activated K^+ currents in adult mouse ventricular myocytes. *J Gen Physiol* 113: 661–678, 1999.
44. **Yagi K, Kim S, Wanibuchi H, Yamashita T, Yamamura Y, Iwao H.** Characteristics of diabetes, blood pressure, and cardiac and renal complications in Otsuka Long-Evans Tokushima Fatty rats. *Hypertension* 29: 728–735, 1997.
45. **Yaras N, Sariahmetoglu M, Bilginoglu A, Aydemir-Koksoy A, Onay-Besikci A, Turan B, Schulz R.** Protective action of doxycycline against diabetic cardiomyopathy in rats. *Br J Pharmacol* 155: 1174–1184, 2008.
46. **Zhao Y, Ransom JF, Li A, Vedantham V, von Drehle M, Muth AN, Tsuchihashi T, McManus MT, Schwartz RJ, Srivastava D.** Dysregulation of cardiogenesis, cardiac conduction, and cell cycle in mice lacking miRNA-1–2. *Cell* 129: 303–317, 2007.
47. **Zhou J, Jeron A, London B, Han X, Koren G.** Characterization of a slowly inactivating outward current in adult mouse ventricular myocytes. *Circ Res* 83: 806–814, 1998.
48. **Zicha S, Xiao L, Stafford S, Cha TJ, Han W, Varro A, Nattel S.** Transmural expression of transient outward potassium current subunits in normal and failing canine and human hearts. *J Physiol* 561: 735–748, 2004.